Biochimica et Biophysica Acta 1840 (2014) 34–40

Contents lists available at ScienceDirect

Biochimica et Biophysica Acta

journal homepage: www.elsevier.com/locate/bbagen

Production of fully assembled and active *Aquifex aeolicus* F_1F_O ATP synthase in *Escherichia coli*

Chunli Zhang [a], Matteo Allegretti [b], Janet Vonck [b], Julian D. Langer [a], Marco Marcia [c], Guohong Peng [a,d,*], Hartmut Michel [a,**]

[a] Max Planck Institute of Biophysics, Department of Molecular Membrane Biology, Max-von-Laue-Str. 3, D-60438 Frankfurt am Main, Germany
[b] Max Planck Institute of Biophysics, Department of Structural Biology, Max-von-Laue-Str. 3, D-60438 Frankfurt am Main, Germany
[c] Department of Molecular, Cellular and Developmental Biology, Yale University, New Haven, CT 06511, USA
[d] Institute of Oceanology, Chinese Academy of Sciences, Qingdao 266071, China

ARTICLE INFO

Article history:
Received 29 May 2013
Received in revised form 13 August 2013
Accepted 27 August 2013
Available online 1 September 2013

Keywords:
Membrane protein complex
Hyperthermophilic organism
Heterologous expression
Artificial operon
Protein assembly
Respiratory enzyme

ABSTRACT

Background: F_1F_O ATP synthases catalyze the synthesis of ATP from ADP and inorganic phosphate driven by ion motive forces across the membrane. A number of ATP synthases have been characterized to date. The one from the hyperthermophilic bacterium *Aquifex aeolicus* presents unique features, i.e. a putative heterodimeric stalk. To complement previous work on the native form of this enzyme, we produced it heterologously in *Escherichia coli*.
Methods: We designed an artificial operon combining the nine genes of *A. aeolicus* ATP synthase, which are split into four clusters in the *A. aeolicus* genome. We expressed the genes and purified the enzyme complex by affinity and size-exclusion chromatography. We characterized the complex by native gel electrophoresis, Western blot, and mass spectrometry. We studied its activity by enzymatic assays and we visualized its structure by single-particle electron microscopy.
Results: We show that the heterologously produced complex has the same enzymatic activity and the same structure as the native ATP synthase complex extracted from *A. aeolicus* cells. We used our expression system to confirm that *A. aeolicus* ATP synthase possesses a heterodimeric peripheral stalk unique among non-photosynthetic bacterial F_1F_O ATP synthases.
Conclusions: Our system now allows performing previously impossible structural and functional studies on *A. aeolicus* F_1F_O ATP synthase.
General significance: More broadly, our work provides a valuable platform to characterize many other membrane protein complexes with complicated stoichiometry, i.e. other respiratory complexes, the nuclear pore complex, or transporter systems.

1. Introduction

F_1F_O ATP synthases are multi-subunit membrane protein complexes that catalyze the synthesis of ATP from ADP and inorganic phosphate driven by ion motive forces across the membrane (H^+ or Na^+) [1–4]. F_1F_O ATP synthases are present in bacteria, mitochondria and chloroplasts and they have been remarkably conserved throughout evolution. The overall enzyme is composed of two distinct subcomplexes. The soluble F_1 subcomplex is formed by the subunits α, β, γ, δ, and ε in a 3:3:1:1:1 stoichiometry. It catalyzes ATP synthesis or hydrolysis following a binding change mechanism [3], according to which three conformational states (open, loose and tight) of the catalytic β subunit alternate during the reaction cycle. The hydrophobic membrane-inserted F_O subcomplex is formed by subunits a, b, and c in 1:2:(8–15) stoichiometry and is the center of ion translocation. Ion-translocation appears to proceed via the so-called "half-channel" pathway by which protons or sodium ions are exchanged at the interface of subunits a and c [5]. Subunits γ and ε form a central stalk and subunits b and δ

Abbreviations: IPTG, isopropyl-β-thiogalactopyranoside; DM, n-decyl-β-D-maltoside; DDM, n-dodecyl-β-D-maltoside; α-PCC, *trans*-4-(*trans*-4′-propylcyclohexyl)cyclohexyl-α-D-maltoside; BN-PAGE, blue native polyacrylamide gel electrophoresis; IMAC, immobilized-metal affinity chromatography; Ni-NTA, Ni–Nitrilotriacetic acid; SEC, size-exclusion chromatography; PMF, peptide mass fingerprint; EM, electron microscopy; LC–ESI–MS, liquid chromatography–electrospray ionization tandem mass spectrometry; MALDI-TOF-MS, matrix-assisted laser desorption-ionization time-of-flight mass spectrometry; AAF_1F_O, *A. aeolicus* ATP synthase isolated from native cells of *A. aeolicus*; EAF_1F_O, *A. aeolicus* ATP synthase heterologously produced in *E. coli*

* Correspondence to: G. Peng, Department of Molecular Membrane Biology, Max Planck Institute of Biophysics, Max-von-Laue Strasse 3, D-60438 Frankfurt am Main, Germany. Tel.: +49 69 6303 1016; fax: +49 69 6303 1002.
** Correspondence to: H. Michel, Department of Molecular Membrane Biology, Max Planck Institute of Biophysics, Max-von-Laue Strasse 3, D-60438 Frankfurt am Main, Germany. Tel.: +49 69 6303 1001; fax: +49 69 6303 1002.
E-mail addresses: Guohong.Peng@biophys.mpg.de (G. Peng), Hartmut.Michel@biophys.mpg.de (H. Michel).

0304-4165/$ – see front matter © 2013 Elsevier B.V. All rights reserved.
http://dx.doi.org/10.1016/j.bbagen.2013.08.023

form a peripheral stalk thus providing a connection between the F_1 and the F_O subcomplexes, and preventing a relative rotation of the α and β subunits and the a subunit.

High resolution structures are available for different parts of the ATP synthase complex, i.e. the bovine F_1 subcomplex [6], c-rings from *Ilyobacter tartaricus*, *Spirulina platensis* and *Bacillus pseudofirmus* OF4 [7–9] and subcomplexes of F_1 and c-rings from yeast [10,11] and bovine mitochondria [12]. The structures of the peripheral stalk of bovine F_1F_O ATP synthase were also determined [13,14]. However, to date, no high resolution structure is available for the entire F_1F_O ATP synthase complex. In particular, structural information is missing for subunit a and therefore the interface between subunit a and c-rings remains to be experimentally characterized. Therefore, for the full understanding of the role of each subunit and of the coupling between ion translocation and rotation, a high-resolution structure of the entire F_1F_O ATP synthase is still required.

Our laboratory has previously reported the biochemical and structural characterization of the F_1F_O ATP synthase isolated from the native membranes of the hyperthermophilic bacterium *Aquifex aeolicus* [15]. To complement such a characterization, expression of *A. aeolicus* F_1F_O ATP synthase in a heterologous genetic system would be very valuable, because it would allow more flexible and feasible genetic and functional studies and because it would open up the possibility to undertake mutagenesis experiments to support further structural investigation.

To date, F_1F_O ATP synthases have been expressed for functional and structural studies both in homologous genetic systems [16–18], as well as in heterologous hosts [19–22]. However, in all cases, the *atp* genes are clustered in a single operon in the source organisms, so that classic recombinant plasmids containing the native *atp* operon were suitable for expression. Instead, in *A. aeolicus*, the nine *atp* genes are not clustered in one operon, but they are distributed over four different genomic loci (Fig. 1), resulting in a total of six different DNA fragments harboring the genes for the nine subunits of the *A. aeolicus* F_1F_O ATP synthase [23]. Moreover, it also needs to be considered that *A. aeolicus* F_1F_O ATP synthase is a large heteromultimeric enzyme of more than 500 kDa in size, with a complex and not yet fully characterized subunit stoichiometry. Therefore the design of a heterologous co-expression vector for the *A. aeolicus* ATP synthase is a challenging task. Nonetheless, in this work we present the successful cloning and expression of all *A. aeolicus* ATP synthase genes in the heterologous host *Escherichia coli* using an artificial operon. Additionally, we report the enzymatic characterization of this complex and its structural properties determined by single-particle electron microscropy (EM). We show that the heterologously produced *A. aeolicus* ATP synthase (hereafter named EAF_1F_O) is active and its structure as determined by single-particle electron microscopy is identical to that of the same complex isolated from native *A. aeolicus* cells (hereafter named AAF_1F_O).

2. Materials and methods

2.1. Protein overproduction and purification

2.1.1. Subcomplex b_1b_2

The subcomplex b_1b_2 was obtained using vector bb2-pTTQ18-A (see Table S2) in the host strain *E. coli* C43(DE3) cultured in 2× YT medium (supplemented with 0.5% (w/v) glucose, 50 μg mL^{-1} carbenicillin). Membranes were prepared and solubilized as described previously [18] with minor modifications (see Supplementary material). The subcomplex b_1b_2 was incubated with Ni–NTA resin (Qiagen) in 20 mM HEPES, pH 7.5, 500 mM NaCl, 20 mM imidazole, 1 mM PMSF, 2% (w/v) DM and eluted by 300 mM imidazole. A final polishing SEC run was performed using a Superdex 200 PC3.2/30 column (GE healthcare) and the SMART system (Pharmacia) in the same buffer.

2.1.2. Subcomplex F_1-αβγ and F_1-αβγε purification

The subcomplexes F_1-αβγ and F_1-αβγε were expressed from vectors pCL11 and pCL12, respectively (see Fig. S3 and Table S2) in the host strain *E. coli* C43(DE3) already containing the pRARE vector. Cells were

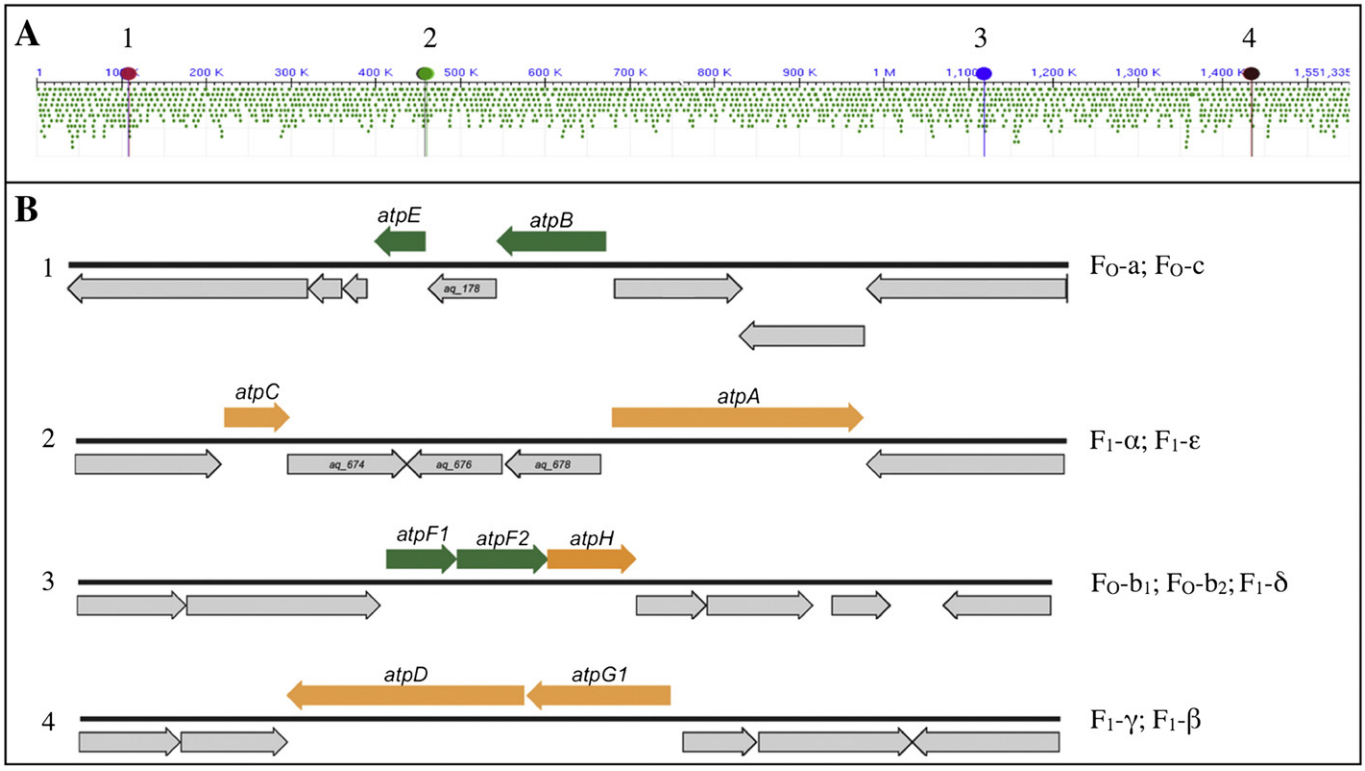

Fig. 1. *Organization of the F_1F_O ATP synthase genes in A. aeolicus.* (A) View of the whole genome of *A. aeolicus*. The nine genes encoding the ATP synthase subunits are split into four loci in the genome. (B) Enlarged view of the four loci. The nine *atp* genes are separated into six DNA fragments located in both the plus and minus DNA strands. Only *atpF1F2H* and *atpDG1* form operons. Genes encoding F_1 subunits are shown in orange, those encoding F_O subunits are shown in green.

cultured in TB medium (supplemented with 50 μg mL^{-1} carbenicillin and 34 μg mL^{-1} chloramphenicol) to a cell density of 0.3–0.4 (OD_{600}), and then induced with 1 mM IPTG and cultured for further 6 h. Proteins from the cytosolic fraction were separated on a Ni–NTA resin following a similar procedure as for subcomplex b_1b_2 but without detergents (see Supplementary material) and polished on a Superdex 200 10/300 GL SEC column (GE healthcare) or a TSK-GEL G4000SW column (TOSOH Bioscience) on an Äkta purifier systems (GE Healthcare).

2.1.3. The EAF_1F_O whole complex

The whole EAF_1F_O complex was expressed from vector pCL21 (see Fig. S3 and Table S2) co-transformed into *E. coli* DK8 with the pRARE plasmid (Novagen). Transformants were selected on LB agar plates containing 50 μg mL^{-1} carbenicillin, 34 μg mL^{-1} chloramphenicol and 30 μg mL^{-1} tetracycline. For protein production, *E. coli* cells were grown in 2× YT medium (supplemented with 50 μg mL^{-1} carbenicillin and 34 μg mL^{-1} chloramphenicol) to a cell density of 0.3–0.4 (OD_{600}), and then induced with 1 mM IPTG and incubated for 6 h. Membranes were prepared (see Supplementary material) and subjected to heat treatment [24], the extract was centrifuged at 200,000 ×*g* for 1 h, the supernatant fraction was incubated at 4 °C for 2 h with Ni–NTA resin, eluted with 150 mM imidazole, and finally purified on a TSK-GEL G4000SW column (TOSOH Bioscience) using Äkta purifier systems (GE Healthcare).

2.2. Antibody production

Polyclonal antibodies (*AQUEA_AtpA*, *AtpC*, *AtpG*) against *A. aeolicus* subunits F_1-α, F_1-ε and F_1-γ were raised in rabbits against chemically synthesized peptides coupled to keyhole limpet hemocyanin (KLH). The peptides used are KEALDAFKQKFVP (*AtpA*), EWEKEAEKARTLLELVEKYR (*AtpC*) and KLSPRDIKRKIQGIKNTKR (*AtpG*), respectively (Thermo Fisher Scientific).

2.3. Protein identification by mass spectrometry

Peptide mass fingerprinting (PMF) and MALDI-TOF experiments were performed as previously described [25] with minor modifications (see Supplementary material).

2.4. Electron microscopy

EAF_1F_O eluted from native PAGE gels was negatively stained with 1% (w/v) uranyl acetate. Electron micrographs were collected using a Philips CM120 (FEI, Eindhoven) at an accelerating voltage of 120 kV under low dose conditions. Images were taken at a magnification of 44,000× on Kodak SO-163 electron image film. The negatives were developed in full-strength D-19 developer for 12 min. Negatives were digitized on a PhotoScan scanner (Z/I Imaging, Aalen, Germany) at a pixel size of 7 μm. Adjacent pixels were averaged to yield a pixel size on the specimen of 4.77 Å. Approximately 2000 particle images were selected using the boxer program from EMAN [26] and aligned, classified and averaged using Imagic V [27].

2.5. Enzymatic activity assays

ATP hydrolysis activity was measured monitoring phosphate production using the LeBel method [28] with minor modifications (see Supplementary material). In-gel ATP hydrolysis assays were performed according to Peters [29] with minor modifications (see Supplementary material).

3. Results

3.1. Heterologous expression strategy for producing EAF_1F_O

The strategy used to produce the *A. aeolicus* ATP synthase in the heterologous host *E. coli* (EAF_1F_O) was aimed at the following goals. By single-gene expression of individual subunits (a, c, γ and ε) and dual-gene expression of specific combinations of different subunits (b_1–b_2, a–c, a–b_1–b_2, γ–ε), we assessed the ability of different host strains to use native operons, native codons, and gene overlaps and to produce functionally active intermediate complexes of the enzyme (for all primers and constructs used see Tables S1 and S2). We determined that subunits b_1 and b_2 form a complex in vitro (see below) and that the membrane components of ATP synthase (subunits a and c) are difficult to produce in isolation, as reported earlier [30,31]. By expressing subcomplexes of the ATP synthase including subunits located in different loci of the *A. aeolicus* genome, i.e. F_1-αβγ (vector pCL11), F_1-αβγε (vector pCL12), and F_O-acb$_1$b$_2$δ (vector pCL02), we assessed the importance of using native intergenic regions. Finally, by combining the genes for F_1-αβγε and for F_O-acb$_1$b$_2$δ (vector pCL21), we were able to produce the entire *A. aeolicus* F_1F_O ATP synthase inlcuding its membrane subunits a and c and to study its structure and function.

3.2. Subcomplex b_1b_2: an *A. aeolicus* native operon with overlapping genes can be recognized in *E. coli*

By expressing subcomplex b_1b_2, we attempted to test (i) whether the native operon *atpF1F2* can be translated into subunits b_1 and b_2 by the heterologous host *E. coli*, and (ii) whether subunits b_1 and b_2 form a complex in *E. coli*. Expression was detected by Western blot analysis from vectors containing different promoters but only a C-terminal and not an N-terminal His_{10}-tag fused to subunit b_2 (see Supplementary material Table S2). The production level was further optimized by screening combinations of different host strains and media at various temperatures, and the highest yield was achieved with vector pTTQ18-A2 [32] using the *E. coli* strain C43(DE3) grown in 2× YT medium and induced by 0.2 mM IPTG at 30 °C for 16 h. Subunits b_1 and b_2 could be solubilized from the *E. coli* membranes by various detergents. The highest yield was obtained using DM, which was thus used for further characterization. Finally, b_1b_2 could be purified to homogeneity as a subcomplex by immobilized metal-ion affinity chromatography (IMAC) and size-exclusion chromatography (SEC) and was stable at 4 °C for at least 5 days (Fig. 2). These results showed that *E. coli* can recognize a native operon of *A. aeolicus* with gene overlaps and that *A. aeolicus* ATP synthase subunits can form a complex in the *E. coli* membranes.

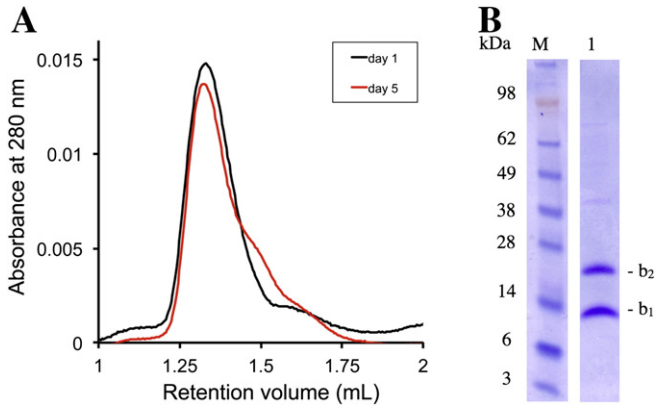

Fig. 2. *The subcomplex b_1b_2.* Subunits b_1 and b_2 were purified as a complex from *E. coli* membranes. (A) Size-exclusion chromatogram in the presence of 0.25% (w/v) DM immediately after purification and after 5-day storage at 4 °C. (B) SDS-PAGE gel of the chromatographic fractions from panel A eluting at 1.3 mL (M is a protein marker, the MW of the marker proteins is shown in kDa on the left of the gel).

3.3. The subcomplexes F_1-αβγ and F_1-αβγε: artificial operons constructed for expression

To test the ability of *E. coli* to express ATP synthase complexes from artificial operons, we cloned the His_6-tagged subcomplexes F_1-αβγ and F_1-αβγε. We chose these subcomplexes because (i) they are soluble and not membrane-inserted, (ii) we could raise polyclonal antibodies against their subunits, and (iii) we could perform enzymatic activity assays to test their functionality.

We tested expression of F_1-αβγ (pCL11 vector) in different host strains with and without the pRARE vector at different temperatures and at different time points after induction by 1 mM IPTG. Under most conditions in which the pRARE vector was used, Western blot analysis indicated the presence of subunit β in whole cell lysates and the maximal levels were obtained in strain C43(DE3) at 37 °C, induced by 1 mM IPTG for 6 h. All three subunits were isolated from the cytoplasmic fraction of the *E. coli* cells and purified in a single IMAC step. The subunits were identified by *in gel* trypsin digestion followed by peptide mass fingerprint (PMF) ESI-MS. The three subunits co-eluted in the same chromatographic fractions indicating that they form a complex in *E. coli* (Figure S1). Furthermore, the complex also showed activity, with a rate of ATP hydrolysis of 1.35 ± 0.14 U/mg.

The pCL11 vector was extended by inserting the *atpC* gene (subunit ε) downstream of gene *atpD* (subunit β), resulting in vector pCL12. The four subunits α, β, γ and ε encoded by pCL12 were successfully expressed and detected by ESI-MS and by Western blot analysis against the corresponding antibodies. The four subunits co-eluted from chromatographic columns indicating that they formed a complex. Finally the F_1-αβγε complex showed an ATP hydrolysis activity of 1.73 ±0.11 U/mg. Besides the fully assembled F_1-subcomplex, BN-PAGE and MS analysis showed the presence of lower order subcomplexes (F_1-$\alpha_2\beta_2$ and F_1-$\alpha_1\beta_1$, Fig. 3), which were inactive in ATP hydrolysis. This result suggests that the minimum ATP hydrolytic unit in *A. aeolicus* ATP synthase probably includes not only subunits α and β, but also subunit γ, as for the *E. coli* ATP synthase [33–35].

3.4. Construction of the artificial operon

Having established that *E. coli* can express functionally active and membrane inserted subcomplexes of ATP synthase from artificial operons, we set out to construct an expression vector to produce the entire ATP synthase complex (EAF_1F_O). The artificial operon was designed to harbor the nine *atp* genes in the order *atpBEF1F2HAGDC*, the same order of the *atp* genes in the native operon from *E. coli*. The construction of the artificial operon included a series of DNA amplifications, manipulation and subcloning (see Fig. S3 and S4) on plasmid pTrc99A, which was selected because it had already been used for production of ATP synthases in the *E. coli* strain DK8 (Δ*atp*) [20–22] (Fig. S5). Briefly, DNA fragments containing the *atp* genes and the corresponding intergenic regions were amplified, modified with unique restriction sites, and subcloned into cloning vector pJET1.2 for DNA propagation and manipulation. Additionally, a His_6-tag (RGSHHHHHH) was inserted at the N-terminus of subunit β by site-directed mutagenesis. Successively, the DNA fragments were sequentially ligated (see Figs. S2, S3, S4, and S5, and Table S3), resulting in the final expression vector pCL21, which contains an operon of 7068 bp. The operon encodes nine *atp* subunits: membrane subunits a, c, b_1, and b_2 and soluble subunits α, β, γ, δ and ε. The individual genes are connected by native intergenic regions derived from the *A. aeolicus* genome, and consisting of the ribosome binding site, the start codon, and the stop codon (See Table S4).

3.5. EAF_1F_O purification from the membranes of E. coli

Expression of EAF_1F_O from pCL21 was tested at various temperatures and time points after induction with 1 mM IPTG, and Western blot analysis revealed the highest levels for His_6-tagged subunit β in *E. coli* membranes when the cells were grown at 37 °C for 6 h after induction. The identification of the soluble subunit β in *E. coli* membranes provided a first hint that the membrane components of the ATP synthase were also expressed and interacted to form a complex. Therefore, we then attempted to purify the ATP synthase complex from *E. coli* membranes to assess whether it was composed of all subunits and whether it was functional.

The optimized purification protocol consisted of the following steps. *E. coli* membranes were solubilized by 3% (w/v) DDM or 3% (w/v) DM, respectively, and subjected to heat treatment, which is a common procedure used to separate thermophilic proteins from the proteins of *E. coli* [24]. After heat treatment, the soluble components of the sample were fractionated by affinity chromatography followed by SEC in the presence of a detergent mixture composed of 0.05% (w/v) DDM + 0.05% (w/v) α-PCC. All subunits co-eluted in the same fractions of the IMAC column, indicating that they formed a membrane complex, which required detergent for assembly and stability (Fig. 4). In the complex, all subunits of EAF_1F_O were detected by PMF ESI-MS (Fig. S7), including membrane subunits a and c, which were not observed in isolation (see above). The EAF_1F_O complex containing all subunits was also observed as a single electrophoretic band on BN-PAGE gels on which EAF_1F_O shows the same electrophoretic mobility as AAF_1F_O. In both preparations subcomplexes corresponding to F_1c_n and $\alpha_1\beta_1$ were also identified by SDS-PAGE and PMF ESI-MS.

3.6. EAF_1F_O catalyzes ATP hydrolysis

First, an *in gel* activity assay at 80 °C was used to directly visualize ATP hydrolysis. With the production of phosphate, lead phosphate precipitation that turned brownish in the presence of Na_2S was directly observed in BN-PAGE gel bands of both fully assembled AAF_1F_O and

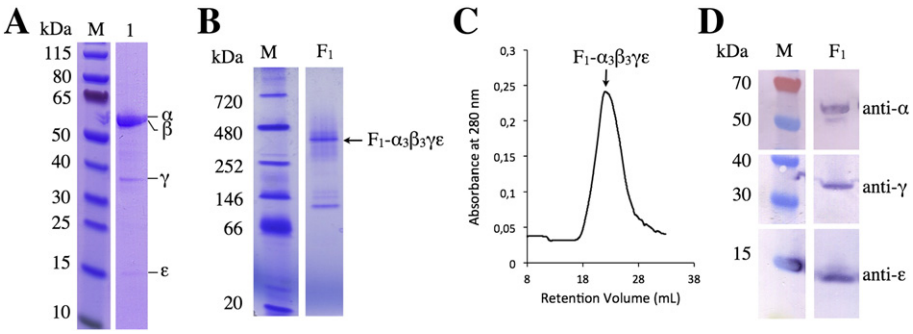

Fig. 3. *Subcomplex F_1-αβγε.* (A) SDS-PAGE gel of subcomplex F_1-αβγε purified by IMAC and SEC. B) BN-PAGE gel of the same sample (the arrow indicates the fully assembled F_1-$\alpha_3\beta_3\gamma\varepsilon$ complex). (C) SEC profile of the fully assembled F_1-$\alpha_3\beta_3\gamma\varepsilon$ complex. The elution peak is indicated by an arrow. (D) Western blot analysis of the SDS-PAGE gel shown in panel A and developed using specific antibodies against subunits α, γ and ε, respectively. In all panels, M is a protein marker and the size of the marker proteins is shown in kDa on the left of the gels.

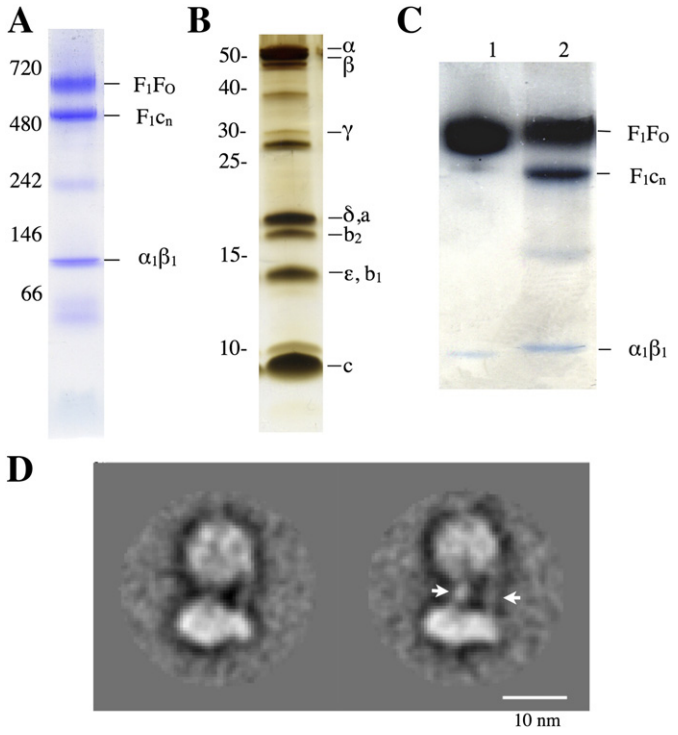

Fig. 4. *The fully assembled and functional EAF$_1$F$_O$.* (A) BN-PAGE gel of the purified EAF$_1$F$_O$ complex. (B) Silver-stained SDS-PAGE of the same sample. (C) In-gel ATP-hydrolysis assay performed on the BN-PAGE gel shown in panel A. Lane 1: AAF$_1$F$_O$, lane 2: EAF$_1$F$_O$. Some activity is also detectable for the subcomplex F$_1$c$_n$. (D) Single-particle electron microscopic reconstruction of the purified EAF$_1$F$_O$ complex. Two class averages are displayed showing that EAF$_1$F$_O$ is fully assembled and identical to AAF$_1$F$_O$ [15]. The peripheral and the central stalks are indicated by the white arrows.

EAF$_1$F$_O$ (Fig. 4). Second, phosphate determination assays were used to compare the ATP hydrolysis activity of AAF$_1$F$_O$ and EAF$_1$F$_O$. At 80 °C, ATP hydrolysis activity of EAF$_1$F$_O$ was 12.77 ± 3.96 U/mg, a value of the same order of magnitude (43%) as that of native AAF$_1$F$_O$ (29.65 ± 3.66 U/mg). Furthermore, the activity was reduced approximately 100 fold (0.17 ± 1.85 U/mg residual activity) by 0.02% (w/v) sodium azide, a common inhibitor of bacterial ATP synthases [36]. These results showed that AAF$_1$F$_O$ and EAF$_1$F$_O$ possess a comparable activity at 80 °C.

3.7. EAF$_1$F$_O$ is fully assembled

To obtain direct structural evidence that EAF$_1$F$_O$ was fully assembled, we used single-particle electron microscopy. After electro-elution from the BN-PAGE, characteristic "mushroom" shaped-particles of EAF$_1$F$_O$ could be observed by single-particle analysis after negative staining. EAF$_1$F$_O$ is ~220 Å long and has two distinct parts. One part possesses a globular shape with a diameter of 110 Å and likely corresponds to the F$_1$ subcomplex. The other part is approximately 100 Å wide parallel to the putative membrane plane and ~60 Å high and likely corresponds to the F$_O$ subcomplex. Importantly, both the central and peripheral stalks are clearly visible in the EM images. Therefore, we conclude that EAF$_1$F$_O$ is fully assembled and shows a similar structural organization as AAF$_1$F$_O$ [15] (Fig. 4).

4. Discussion

4.1. The strategy for the heterologous expression of A. aeolicus ATP synthase in E. coli

To obtain the nine-subunit *A. aeolicus* ATP synthase complex in *E. coli*, two different strategies could theoretically be used, namely (i) production of the individual subunits followed by in vitro reconstitution [24,35], or (ii) co-production of all the subunits in the same host. However, in practice, the first strategy is not applicable for the ATP synthase complex, because certain subunits (i.e. subunit a) cannot be produced well or at all in isolation (see Section 3, Results and [30,31]). Therefore, the second strategy had to be followed.

Little is known about transcription, translation and assembly of the *A. aeolicus* F$_1$F$_O$ ATP synthase in native *A. aeolicus* cells, but these processes must be rather complex in respect to other organisms because the *atp* genes are dispersed to four loci throughout the *A. aeolicus* genome. The *E. coli* F$_1$F$_O$ ATP synthase is better-known and extensive studies have been carried out to understand its expression and assembly [35]. The *atp* operon of *E. coli* comprises nine genes ordered *atpIBEFHAGDC* [37,38]. It has a single major promoter which initiates transcription 73 bp upstream of the start codon of gene I (*atpI*) [39–43]. The *atp* operon is transcribed to produce a single, large polycistronic mRNA containing all nine cistrons, which are then translated at different rates to match the F$_1$F$_O$ ATP synthase stoichiometry [44,45]. Furthermore, recombinant *E. coli* F$_1$F$_O$ ATP synthase was overproduced homologously in the *E. coli* DK8 (Δ*atp*) strain [46] with a recombinant plasmid containing the entire *atp* operon [18,47]. The *E. coli* DK8 strain (Δ*atp*) was also used as a host strain for producing heterologously recombinant F$_1$-$\alpha_3\beta_3\gamma$ of *Bacillus* PS3 [19], the entire F$_1$F$_O$ complexes of *I. tartaricus* [20], *C. thermarum* TA2.A1 [21] and *Acetobacterium woodii* [22].

Because *E. coli* is well studied, and because it was used successfully for so many other ATP synthases, we chose it as a host organism also for our study. Given that *A. aeolicus* does not possess one *atp* operon, we preferred to design an artificial operon as similar as possible to the *E. coli* native one, rather than co-expressing the genes from several expression vectors [48]. A number of limitations had to be taken into account for obtaining successful production and correct assembly of the whole complex. (i) Genes for different isoforms of various subunits are present in the *A. aeolicus* genome [23]. We included in our artificial operon only isoforms that are known to be present in the mature ATP synthase in native cells [15,49], i.e. genes *atpF1* and *atpF2* encoding subunits b$_1$ and b$_2$ but not gene *atpG2* encoding an isoform of subunit γ. We also did not include any *atpI* gene, because *A. aeolicus* is not known to possess homologues of this gene (see Supplementary material). (ii) ATP synthase is a heteromultimeric complex in which the correct stoichiometry of all subunits needs to be carefully regulated. We regulated the stoichiometry of EAF$_1$F$_O$ by accurate selection of the translation initiation regions (TIRs). We used complete TIRs from the *A. aeolicus* genes, including 30 bp upstream of the start codon of six genes, *atpB*, *atpE*, *atpF1*, *atpA*, *atpG* and *atpC* and limiting as much as possible all modifications of TIRs affecting the intercistronic distance between neighboring genes (see Supplementary material and Tables S3 and S4). (iii) The mean difference of codon usage between *E. coli* and *A. aeolicus* is 30.91%. We avoided codon usage bias by increasing the copy number of the tRNAs specific for rare codons using the commercial pRARE vector (Novagen, see Supplementary material and Fig. S6). (iv) *A. aeolicus* ATP synthase is characterized by the presence of overlaps in genes *atpF1*, *atpF2* and *atpH*. Our tests suggest that such overlaps can be recognized by *E. coli* to coordinate gene expression of subunits b$_1$, b$_2$ and δ, in line with previous reports [21] (see Section 3, Results and Supplementary material).

4.2. Heterologous expression was decisive to discover new properties of A. aeolicus F$_1$F$_O$ ATP synthase

Using the expression strategy described, we were able to produce *A. aeolicus* ATP synthase heterologously in *E. coli* with a yield of approximately 0.06–0.15 mg of pure EAF$_1$F$_O$ per liter of cell culture (or 0.03 mg EAF$_1$F$_O$ per gram of *E. coli* wet cell pellet). This yield is comparable to that obtained for F$_1$F$_O$ ATP synthase of *I. tartaricus* heterologously produced in *E. coli* [50], and slightly lower than that obtained for homologously recombinant V$_1$V$_O$ ATP synthase from *T. thermophilus* (0.15 mg V$_1$V$_O$ ATP synthase per gram of wet cell pellet) [51]. While

expression is still low for crystallographic studies, it did allow us to undertake biochemical, enzymatic and biophysical studies and to discover new properties of *A. aeolicus* ATP synthase.

First, our biochemical investigation enabled us to define the properties of certain ATP synthase subunits, which present unique features in *A. aeolicus*. For instance, using the EAF_1F_O construct described in this work, we discovered that subunit c requires an N-terminal signal peptide for expression and membrane insertion [52]. The signal peptide – which is an obligatory component of our artificial operon – is successively cleaved off from the mature ATP synthase [52]. Such a feature is to date unique within F-type ATP synthases and led us to identify a new phylogenetic group of ATP synthases, mostly populated by enzymes of thermophilic species and possibly possessing unique properties that determine membrane insertion and assembly [52]. Considering that the *A. aeolicus* subunit c could not be obtained in isolation (see above), the study of its N-terminal properties would not have been possible without the heterologous expression of EAF_1F_O. Besides the properties of subunit c, our work also sheds light on the properties of subunits b_1 and b_2. Previously these subunits were co-identified in the pure AAF_1F_O [15], but their mode of association in the enzyme complex was unclear. Our heterologous expression study now clarifies that subunits b_1 and b_2 can associate to form a complex in vitro and thus corroborates the previous hypothesis that *A. aeolicus* ATP synthase possesses a heterodimeric peripheral stalk and is therefore unique among ATP synthases of non-photosynthetic organisms [15].

Second, our enzymatic studies proved that the ATP hydrolysis activity of the pure EAF_1F_O is comparable to that of the pure AAF_1F_O at 80 °C. In general, the rate of ATP hydrolysis of EAF_1F_O and AAF_1F_O is in the same range as that of the F_1F_O ATP synthase from *E. coli* [18]. EAF_1F_O is actually slightly less active than AAF_1F_O (43%), but such a trend is not unusual when comparing the activity of heterologously produced vs native enzymes. For instance, the F_1F_O ATP synthase of *I. tartaricus* is ~3 fold less active when produced heterologously in *E. coli* [50] in respect to the same enzyme isolated from native cells [53]. Certainly, monitoring the reaction of ATP synthesis and the rates of proton translocation will be necessary in the future to complete the comparison between AAF_1F_O and EAF_1F_O. However, our results already open the way to previously impossible functional studies on *A. aeolicus* ATP synthase, i.e. by site-directed mutagenesis, cell viability studies, in vivo complementation experiments and in vitro enzymatic assays.

Third, our single-particle EM reconstruction shows that EAF_1F_O has an identical structure to AAF_1F_O. AAF_1F_O is 230 Å long, its globular F_1 subcomplex possesses a diameter of 110 Å, and the c-ring in the F_O subcomplex is ~90 Å wide and ~70 Å high [15]. These dimensions match well with those measured for EAF_1F_O (Fig. 4). More importantly, the AAF_1F_O single-particle reconstruction shows much stronger signal for its peripheral stalk subunits b_1 and b_2 [15] than F_1F_O ATP synthases from other bacteria, e.g. *E. coli* [54] and *C. thermarum* strain TA2.A1 [55]. In this work, we observe the same strong signal for subunits b_1 and b_2 in EAF_1F_O, suggesting that in respect to other ATP synthases the peripheral stalk is more rigid and it remains intact during purification in *A. aeolicus* ATP synthase, independent if the enzyme is produced from native source or heterologously. This observation makes *A. aeolicus* ATP synthase a promising candidate for studies aiming to determine the structure of the intact enzyme. Finally, obtaining an identical EM signal for EAF_1F_O and AAF_1F_O is a crucial result because it opens up the way for experiments aiming to analyze the unique structural features previously observed in *A. aeolicus* ATP synthase [15]. For instance, by site-directed mutagenesis or using tags and specific antibodies, it will be possible to determine if there is a direct connection between the peripheral stalk and subunit δ [15], and whether the tilts and kinks previously observed for the central stalk [15,56] are functionally relevant.

In conclusion, the successful production of the fully assembled and active F_1F_O ATP synthase from *A. aeolicus* in *E. coli* reported in this work provides a valuable and novel genetic system to study *A. aeolicus* F_1F_O ATP synthase. To a broader extent, it will also serve in the future as a solid reference for designing strategies aimed at producing large multi-subunit complexes with complicated stoichiometry.

Acknowledgements

We thank Dr. Thomas Meier for kindly providing the pTrc99A vector and *E. coli* DK8 strain, Imke Wuellenweber for preparing the ESI-TOF samples, Cornelia Münke for the preparation of the modified vectors pET-G, Laura Preiss for detailed discussion, and Tanja Hedderich and Jennifer Witt for excellent technical assistance. This work was supported by the Deutsche Forschungsgemeinschaft (SFB 472), the Max Planck Gesellschaft, the Cluster of Excellence "Macromolecular Complexes" (Frankfurt am Main, Germany), and the International Max Planck Research School on Structure and Function of Biological Membranes (Frankfurt am Main, Germany). We declare no conflict of interest.

Appendix A. Supplementary data

Supplementary data to this article can be found online at http://dx.doi.org/10.1016/j.bbagen.2013.08.023.

References

[1] P. Mitchell, J. Moyle, Stoichiometry of proton translocation through the respiratory chain and adenosine triphosphatase systems of rat liver mitochondria, Nature 208 (1965) 147–151.
[2] W. Hilpert, B. Schink, P. Dimroth, Life by a new decarboxylation-dependent energy conservation mechanism with Na as coupling ion, EMBO J. 3 (1984) 1665–1670.
[3] P.D. Boyer, The ATP synthase—a splendid molecular machine, Annu. Rev. Biochem. 66 (1997) 717–749.
[4] P. Dimroth, C. von Ballmoos, T. Meier, G. Kaim, Electrical power fuels rotary ATP synthase, Structure 11 (2003) 1469–1473.
[5] W. Junge, H. Lill, S. Engelbrecht, ATP synthase: an electrochemical transducer with rotatory mechanics, Trends Biochem. Sci. 22 (1997) 420–423.
[6] J.P. Abrahams, A.G. Leslie, R. Lutter, J.E. Walker, Structure at 2.8 A resolution of F-$_1$-ATPase from bovine heart mitochondria, Nature 370 (1994) 621–628.
[7] T. Meier, P. Polzer, K. Diederichs, W. Welte, P. Dimroth, Structure of the rotor ring of F-Type Na^+-ATPase from *Ilyobacter tartaricus*, Science 308 (2005) 659–662.
[8] D. Pogoryelov, O. Yildiz, J.D. Faraldo-Gomez, T. Meier, High-resolution structure of the rotor ring of a proton-dependent ATP synthase, Nat. Struct. Mol. Biol. 16 (2009) 1068–1073.
[9] L. Preiss, O. Yildiz, D.B. Hicks, T.A. Krulwich, T. Meier, A new type of proton coordination in an F(1)F(o)-ATP synthase rotor ring, PLoS Biol. 8 (2010) e1000443.
[10] D. Stock, A.G. Leslie, J.E. Walker, Molecular architecture of the rotary motor in ATP synthase, Science 286 (1999) 1700–1705.
[11] A. Dautant, J. Velours, M.F. Giraud, Crystal structure of the Mg.ADP-inhibited state of the yeast F_1c_{10}-ATP synthase, J. Biol. Chem. 285 (2010) 29502–29510.
[12] I.N. Watt, M.G. Montgomery, M.J. Runswick, A.G.W. Leslie, J.E. Walker, Bioenergetic cost of making an adenosine triphosphate molecule in animal mitochondria, Proc. Natl. Acad. Sci. U. S. A. 107 (2010) 16823–16827.
[13] D.M. Rees, A.G. Leslie, J.E. Walker, The structure of the membrane extrinsic region of bovine ATP synthase, Proc. Natl. Acad. Sci. U. S. A. 106 (2009) 21597–21601.
[14] V.K. Dickson, J.A. Silvester, I.M. Fearnley, A.G. Leslie, J.E. Walker, On the structure of the stator of the mitochondrial ATP synthase, EMBO J. 25 (2006) 2911–2918.
[15] G. Peng, M. Bostina, M. Radermacher, I. Rais, M. Karas, H. Michel, Biochemical and electron microscopic characterization of the F_1F_0 ATP synthase from the hyperthermophilic eubacterium *Aquifex aeolicus*, FEBS Lett. 580 (2006) 5934–5940.
[16] Y. Moriyama, A. Iwamoto, H. Hanada, M. Maeda, M. Futai, One-step purification of *Escherichia coli* H^+-ATPase F_0F_1 and its reconstitution into liposomes with neurotransmitter transporters, J. Biol. Chem. 266 (1991) 22141–22146.
[17] T.M. Duncan, V.V. Bulygin, Y. Zhou, M.L. Hutcheon, R.L. Cross, Rotation of Subunits during Catalysis by *Escherichia coli* F_1-Atpase, Proc. Natl. Acad. Sci. U. S. A. 92 (1995) 10964–10968.
[18] R.R. Ishmukhametov, M.A. Galkin, S.B. Vik, Ultrafast purification and reconstitution of His-tagged cysteine-less *Escherichia coli* F_1F_s ATP synthase, Biochim. Biophys. Acta 1706 (2005) 110–116.
[19] T. Matsui, M. Yoshida, Expression of the wild-type and the Cys-/Trp-less alpha 3 beta 3 gamma complex of thermophilic F1-ATPase in *Escherichia coli*, Biochim. Biophys. Acta 1231 (1995) 139–146.
[20] J.K. Hakulinen, A.L. Klyszejko, J. Hoffmann, L. Eckhardt-Strelau, B. Brutschy, J. Vonck, T. Meier, Structural study on the architecture of the bacterial ATP synthase F_o motor, Proc. Natl. Acad. Sci. U. S. A. 109 (2012) E2050–E2056.
[21] D.G. McMillan, S. Keis, P. Dimroth, G.M. Cook, A specific adaptation in the a subunit of thermoalkaliphilic F_1F_O-ATP synthase enables ATP synthesis at high pH but not at neutral pH values, J. Biol. Chem. 282 (2007) 17395–17404.
[22] K. Brandt, D.B. Muller, J. Hoffmann, C. Hubert, B. Brutschy, G. Deckers-Hebestreit, V. Muller, Functional production of the Na^+ F_1F_O ATP synthase from *Acetobacterium woodii* in *Escherichia coli* requires the native Atpl, J. Bioenerg. Biomembr. 45 (2013) 15–23.

[23] G. Deckert, P.V. Warren, T. Gaasterland, W.G. Young, A.L. Lenox, D.E. Graham, R. Overbeek, M.A. Snead, M. Keller, M. Aujay, R. Huber, R.A. Feldman, J.M. Short, G.J. Olsen, R.V. Swanson, The complete genome of the hyperthermophilic bacterium *Aquifex aeolicus*, Nature 392 (1998) 353–358.
[24] H. Imamura, S. Funamoto, M. Yoshida, K. Yokoyama, Reconstitution in vitro of V_1 complex of *Thermus thermophilus* V-ATPase revealed that ATP binding to the A subunit is crucial for V_1 formation, J. Biol. Chem. 281 (2006) 38582–38591.
[25] M. Marcia, J.D. Langer, D. Parcej, V. Vogel, G. Peng, H. Michel, Characterizing a monotopic membrane enzyme. Biochemical, enzymatic and crystallization studies on *Aquifex aeolicus* sulfide:quinone oxidoreductase, Biochim. Biophys. Acta 1798 (2010) 2114–2123.
[26] S.J. Ludtke, P.R. Baldwin, W. Chiu, EMAN: semiautomated software for high-resolution single-particle reconstructions, J. Struct. Biol. 128 (1999) 82–97.
[27] M. van Heel, G. Harauz, E.V. Orlova, R. Schmidt, M. Schatz, A new generation of the IMAGIC image processing system, J. Struct. Biol. 116 (1996) 17–24.
[28] D. LeBel, G.G. Poirier, A.R. Beaudoin, A convenient method for the ATPase assay, Anal. Biochem. 85 (1978) 86–89.
[29] J.M. Peters, J.R. Harris, A. Lustig, S. Muller, A. Engel, S. Volker, W.W. Franke, Ubiquitous soluble Mg(2+)-ATPase complex. A structural study, J. Mol. Biol. 223 (1992) 557–571.
[30] K. von Meyenburg, B.B. Jorgensen, O. Michelsen, L. Sorensen, J.E. McCarthy, Proton conduction by subunit a of the membrane-bound ATP synthase of *Escherichia coli* revealed after induced overproduction, EMBO J. 4 (1985) 2357–2363.
[31] I. Arechaga, B. Miroux, M.J. Runswick, J.E. Walker, Over-expression of *Escherichia coli* F_1F_o-ATPase subunit a is inhibited by instability of the *uncB* gene transcript, FEBS Lett. 547 (2003) 97–100.
[32] S. Surade, M. Klein, P.C. Stolt-Bergner, C. Muenke, A. Roy, H. Michel, Comparative analysis and "expression space" coverage of the production of prokaryotic membrane proteins for structural genomics, Protein Sci. 15 (2006) 2178–2189.
[33] B.J. Koebmann, H.V. Westerhoff, J.L. Snoep, D. Nilsson, P.R. Jensen, The glycolytic flux in *Escherichia coli* is controlled by the demand for ATP, J. Bacteriol. 184 (2002) 3909–3916.
[34] A.E. Senior, A. Muharemagic, S. Wilke-Mounts, Assembly of the stator in *Escherichia coli* ATP synthase. Complexation of alpha subunit with other F1 subunits is prerequisite for delta subunit binding to the N-terminal region of alpha, Biochemistry 45 (2006) 15893–15902.
[35] M. Futai, T. Noumi, M. Maeda, Molecular genetics of F_1-ATPase from *Escherichia coli*, J. Bioenerg. Biomembr. 20 (1988) 41–58.
[36] M.W. Bowler, M.G. Montgomery, A.G. Leslie, J.E. Walker, How azide inhibits ATP hydrolysis by the F-ATPases, Proc. Natl. Acad. Sci. U. S. A. 103 (2006) 8646–8649.
[37] H. Kanazawa, M. Futai, Structure and function of H^+-ATPase: what we have learned from *Escherichia coli* H^+-ATPase, Ann. N. Y. Acad. Sci. 402 (1982) 45–64.
[38] J.E. Walker, M. Saraste, N.J. Gay, The *unc* operon. Nucleotide sequence, regulation and structure of ATP-synthase, Biochim. Biophys. Acta 768 (1984) 164–200.
[39] K. von Meyenburg, B.B. Jorgensen, J. Nielsen, F.G. Hansen, Promoters of the *atp* operon coding for the membrane-bound ATP synthase of *Escherichia coli* mapped by Tn10 insertion mutations, Mol. Gen. Genet. MGG 188 (1982) 240–248.
[40] A.C. Porter, W.S. Brusilow, R.D. Simoni, Promoter for the *unc* operon of *Escherichia coli*, J. Bacteriol. 155 (1983) 1271–1278.
[41] J. Nielsen, B.B. Jorgensen, K.V. van Meyenburg, F.G. Hansen, The promoters of the atp operon of *Escherichia coli* K12, Mol. Gen. Genet. MGG 193 (1984) 64–71.
[42] H. Kanazawa, K. Mabuchi, T. Kayano, T. Noumi, T. Sekiya, M. Futai, Nucleotide sequence of the genes for F_0 components of the proton-translocating ATPase from *Escherichia coli*: prediction of the primary structure of F_0 subunits, Biochem. Biophys. Res. Commun. 103 (1981) 613–620.
[43] H.M. Jones, C.M. Brajkovich, R.P. Gunsalus, In vivo 5′ terminus and length of the mRNA for the proton-translocating ATPase (*unc*) operon of *Escherichia coli*, J. Bacteriol. 155 (1983) 1279–1287.
[44] J.E. McCarthy, H.U. Schairer, W. Sebald, Translational initiation frequency of *atp* genes from *Escherichia coli*: identification of an intercistronic sequence that enhances translation, EMBO J. 4 (1985) 519–526.
[45] J.E. McCarthy, Expression of the *unc* genes in *Escherichia coli*, J. Bioenerg. Biomembr. 20 (1988) 19–39.
[46] D.J. Klionsky, W.S. Brusilow, R.D. Simoni, In vivo evidence for the role of the epsilon subunit as an inhibitor of the proton-translocating ATPase of *Escherichia coli*, J. Bacteriol. 160 (1984) 1055–1060.
[47] H. Noji, K. Hasler, W. Junge, K. Kinosita Jr., M. Yoshida, S. Engelbrecht, Rotation of *Escherichia coli* F(1)-ATPase, Biochem. Biophys. Res. Commun. 260 (1999) 597–599.
[48] N.H. Tolia, L. Joshua-Tor, Strategies for protein coexpression in *Escherichia coli*, Nat. Methods 3 (2006) 55–64.
[49] M. Guiral, L. Prunetti, S. Lignon, R. Lebrun, D. Moinier, M.T. Giudici-Orticonit, New insights into the respiratory chains of the chemolithoautotrophic and hyperthermophilic bacterium *Aquifex aeolicus*, J. Proteome Res. 8 (2009) 1717–1730.
[50] J. Hakulinen, Biochemical and structural investigations on architecture of the F_O complex from *Ilyobacter tartaricus* ATP synthase, Ph.D. Theses Max-Planck-Insitute of biophysics, Frankfurt, Germany, 2012.
[51] K. Yokoyama, K. Nagata, H. Imamura, S. Ohkuma, M. Yoshida, M. Tamakoshi, Subunit arrangement in V-ATPase from *Thermus thermophilus*, J. Biol. Chem. 278 (2003) 42686–42691.
[52] C. Zhang, M. Marcia, J.D. Langer, G. Peng, H. Michel, Role of the N-terminal signal peptide in the membrane insertion of *Aquifex aeolicus* F_1F_0 ATP synthase c-subunit, FEBS J. 280 (2013) 3425–3435.
[53] S. Neumann, U. Matthey, G. Kaim, P. Dimroth, Purification and properties of the F1Fo ATPase of *Ilyobacter tartaricus*, a sodium ion pump, J. Bacteriol. 180 (1998) 3312–3316.
[54] B. Bottcher, I. Bertsche, R. Reuter, P. Graber, Direct visualisation of conformational changes in EF(0)F(1) by electron microscopy, J. Mol. Biol. 296 (2000) 449–457.
[55] D. Matthies, S. Haberstock, F. Joos, V. Dotsch, J. Vonck, F. Bernhard, T. Meier, Cell-free expression and assembly of ATP synthase, J. Mol. Biol. 413 (2011) 593–603.
[56] A. Stocker, S. Keis, J. Vonck, G.M. Cook, P. Dimroth, The structural basis for unidirectional rotation of thermoalkaliphilic F1-ATPase, Structure 15 (2007) 904–914.